

PROPERTIES OF H<sup>-</sup> and D<sup>-</sup> BEAMS FROM MAGNETRON AND PENNING SOURCES\*

Th. Sluyters and V. Kovarik  
 Brookhaven National Laboratory  
 Upton, N. Y.

Summary

The quality of negative hydrogen isotope beams are evaluated after extraction from magnetron and Penning sources. The general conclusions of these measurements are: (A) the beam quality from these plasma sources are adequate for the transport of high current negative ion beams in bending magnets; (B) there is evidence of practically complete space-charge neutralization in the drift space beyond the extractor; (C) the beam performance from the Penning source appears to be better than that of the magnetron source, and (D) it is likely that the high electric field gradient and a concave ion emission boundary are responsible for a beam cross-over near the anode aperture, which causes beam divergence practically independent of the extraction geometry.

Introduction and Experimental Results

For the design of an H<sup>-</sup> beam transport and acceleration system, it is necessary to know the beam quality, i.e. the current density distribution and the emittance in the (x, x') and (y, y') phase planes.

The density distribution and emittances were automatically measured and analyzed by an on-line mini-computer<sup>1</sup> and two emittance monitors: one for the horizontal (x, x') emittance and the other for the vertical (y, y') emittance. Each monitor head consists of a 0.004" sample slit and 30 Faraday cups (Fig. 1). The angle resolution is 25 mrad/cup. The monitors, located at 4 or 8 cm. from the source, move in steps of 0.016" to 0.040" per pulse. The computer graphics displays: (A) the emittance in two-dimensional phase-space, (B) the emittance values as a function of threshold level, (C) the density distribution, and (D) the emittance in a three-dimensional plot in which the third coordinate is the beam intensity.

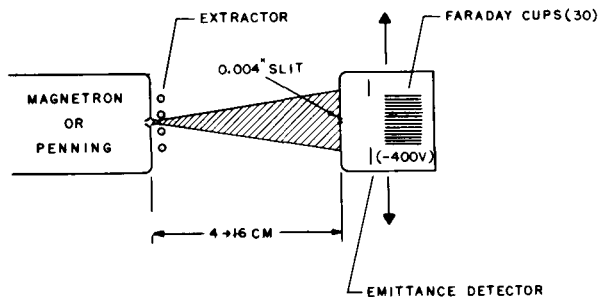


Fig. 1 Experimental arrangement

\*Work done under the auspices of the U.S. Department of Energy

The studies were carried out with three types of source covers and a single extractor grid. Their configurations are sketched in Fig. 2.

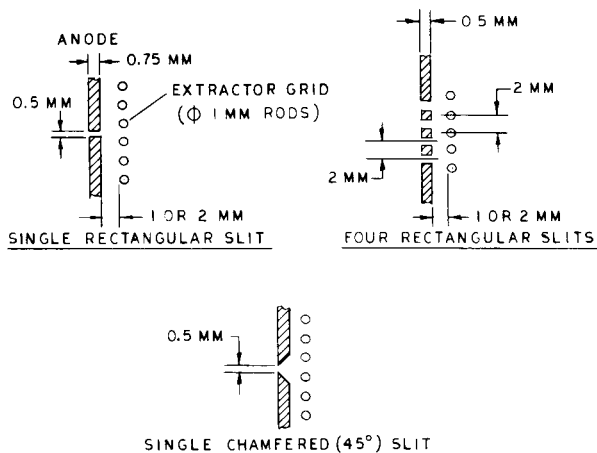


Fig. 2 Emission slit and extractor configurations

Some typical computer output displays are shown in Figs. 3, 4, 5, 6, and 7. Only the display in Fig. 5 was obtained with the monitor at 4 cm from the source. Table I summarizes parameters of several measurements for Penning and magnetron sources, for single slit and four slits. The slit configuration is either rectangular or chamfered.

Discussion

The emittance measurements for beam currents up to 0.35 A, show that the divergence of the negative ion beam perpendicular to the slits is between ±200 and 275 milliradian for energies up to 11 keV. The divergence in the direction of the slits is between ±75 and 125 milliradian.

Measurements also indicate that the angle of the beam envelope does not change in the drift space beyond 4 cm downstream of the source. Figure 5 is the emittance of a 0.2 A beam from a Penning source with four emission slits. All four beams are separated in phase-space. Tracing these beams back to the extractor slit without space charge, the width of each beamlet is very close to that of the aperture, which is 1 mm. These results suggest that for the measured current densities of up to about 1A/cm<sup>2</sup> and background pressure of about 10<sup>-4</sup> Torr, space charge does not play an important role in the drift space beyond the extractor. The divergence of the beam is then determined: (A) by the optics of the extraction system, including the magnetic field and the space charge of the beam in and around the extraction region and (B) by the initial ion emitting surface. Figure 8 shows

TABLE I

Penning Source (Slit dimension 0.5 x 25 mm<sup>2</sup>)

SCAN DIRECTION AND SLIT GEOMETRY	BEAM CURRENT [A]	EMISSION CURRENT DENSITY [A/cm]	LINEAR CURRENT DENSITY [A/cm]	ENERGY [keV]	Hydrogen			CATHODE POWER DENSITY [kW/cm]	CROSS-OVER WIDTH [mm]	ARC I [A]	ARC V [V]
					H.V. GRADIENT [kV/cm]	EMITTANCE [cm-mrad]	MAX [mrad]				
↓Slit(1, rect.)	0.1	0.8	0.04	7.5	75	208 (82%)	260	8.0	5.0	100	160
↓Slit(1, chamf.)	0.125	1.0	0.05	10.0	100	110 (80%)	200	6.4	3.6	80	160
↓Slit(4, rect.)	0.3	0.6	0.12	10.5	52	353 (85%)	200	12.0	10.0	300	80
↑Slit(1, rect.)	0.1	0.8	0.04	8.5	85	600 (82%)	160	8.8	17.0	110	160
↑Slit(1, chamf.)	0.09	0.7	0.04	7.5	75	520 (75%)	80	7.2	26.0	60	240
↑Slits(4, rect.)	0.3	0.6	0.12	10.5	52	450 (85%)	100	11.0	26.0	220	100

Deuterium											
SCAN DIRECTION AND SLIT GEOMETRY	BEAM CURRENT [A]	EMISSION CURRENT DENSITY [A/cm]	LINEAR CURRENT DENSITY [A/cm]	ENERGY [keV]	H.V. GRADIENT [kV/cm]	EMITTANCE [cm-mrad]	MAX [mrad]	CATHODE POWER DENSITY [kW/cm]	CROSS-OVER WIDTH [mm]	ARC I [A]	ARC V [V]
↓Slit(1, chamf.)	0.11	0.88	0.04	11.3	66	227 (87%)	250	12.2	5.8	350	70
↓Slit(4, rect.)	0.22	0.44	0.09	10.0	50	296 (85%)	210	10.0	9.0	200	100

Magnetron (slit dimension 0.5 x 43 mm<sup>2</sup>)

SOURCE AND SLIT GEOMETRY	BEAM CURRENT [A]	EMISSION CURRENT DENSITY [A/cm]	LINEAR CURRENT DENSITY [A/cm]	ENERGY [keV]	Hydrogen			CATHODE POWER DENSITY [kW/cm]	CROSS-OVER WIDTH [mm]	ARC I [A]	ARC V [V]
					H.V. GRADIENT [kV/cm]	EMITTANCE [cm-mrad]	MAX [mrad]				
↓Slit(1, rect.)	0.2	0.9	0.05	8.5	85	250 (85%)	275	2.3	5.5	140	200
↓Slit(1, chamf.)	0.2	1.0	0.05	11.0	110	290 (85%)	275	1.8	7.0	150	150
↓Slit(4, rect.)	0.25	0.3	0.06	9.5	48	380 (85%)	210	2.5	7.7	140	220
↑Slit(1, rect.)	0.35	1.6	0.08	10.0	100	600 (75%)	75	2.6	4.3	160	200
↑Slit(4, rect.)	0.25	0.3	0.06	7.0	35	600 (80%)	90	2.3	4.3	140	200

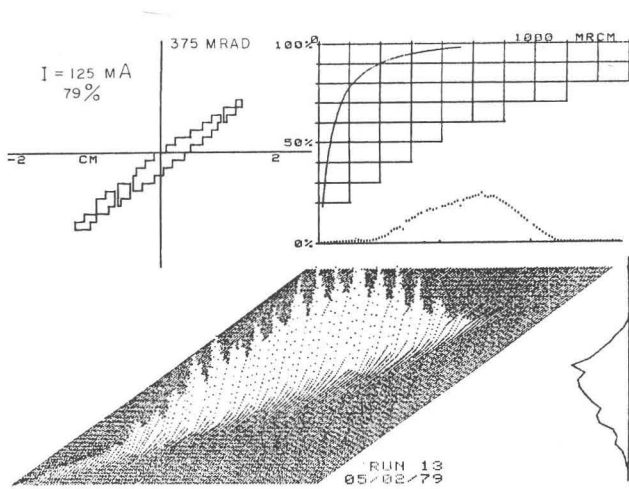


Fig. 3 Penning emittance perpendicular to single emission slit

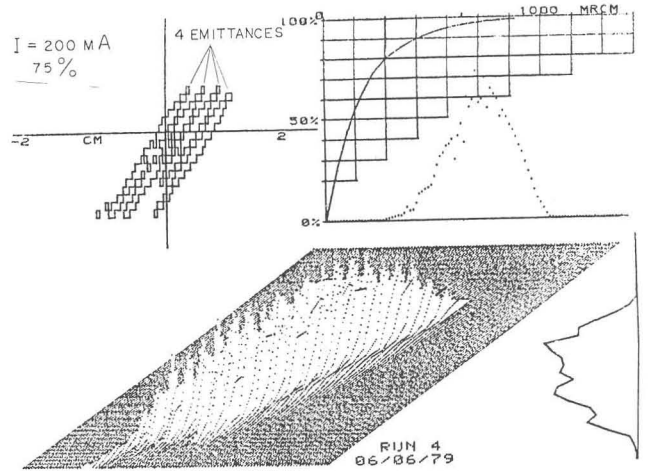


Fig. 5 Penning emittance perpendicular to 4 emission slits

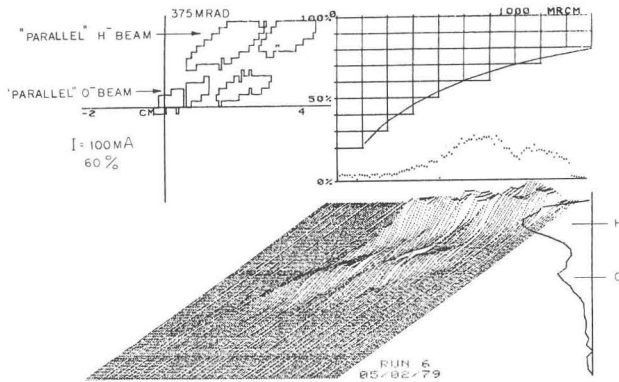


Fig. 4 Penning emittance parallel to single emission slit

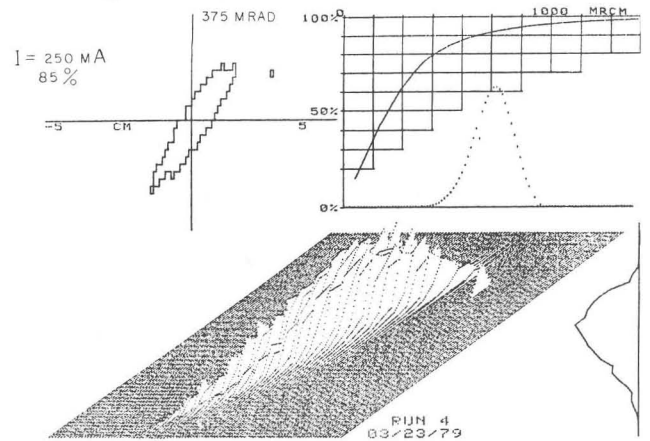


Fig. 6 Magnetron emittance perpendicular to 4 emission slits

the envelope of a negative ion beam with a density of  $0.5 \text{ A/cm}^2$ , calculated with the SLAC Electron Trajectory Program (SLAC 166) for a field gradient

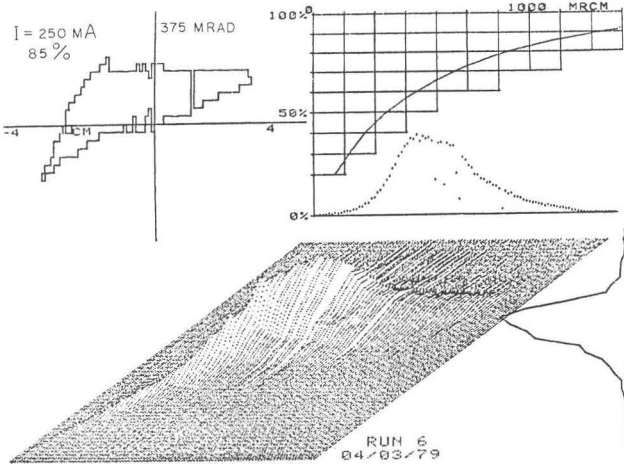


Fig. 7 Magnetron emittance parallel to 4 emission slits

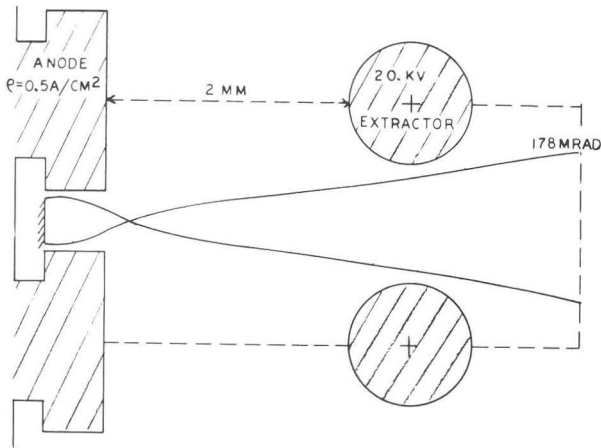


Fig. 8 Beam envelope for an ion beam of  $0.5 \text{ A/cm}^2$

of  $50 \text{ kV/cm}$  and taking into account space charge. This calculation suggests that even for a flat emission boundary at the inside plane of the anode, there is strong over-focusing of the beam. The particles are intercepted either at the anode slit or at the extractor electrode. Reduction of extraction voltage should, in principle, move the cross-over point downstream; however, lower extraction voltage also changes the trajectories in the slit region and the final beam divergence remains practically the same (see Fig. 9). Without taking into account what actually happens at the plasma boundary, it is clear that the beam optics should be a compromise between the need for high gradients to extract an intense beam and for low gradients to attain a more parallel beam.

Providing a  $45^\circ$  chamfer on the anode slit reduces the electrostatic shadowing, allowing the extraction field to penetrate deeper into the slit, alleviating some space-charge dilation and blockage. Figure 10 demonstrates the different beam trajectories expected with and without a  $45^\circ$  chamfered anode slit, assuming a flat plasma boundary.

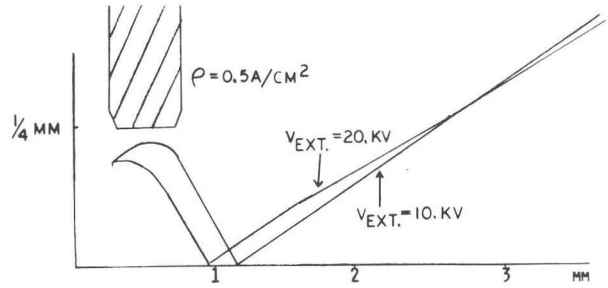


Fig. 9 Beam envelopes for 10 and 20 kV extraction with rectangular emission slit

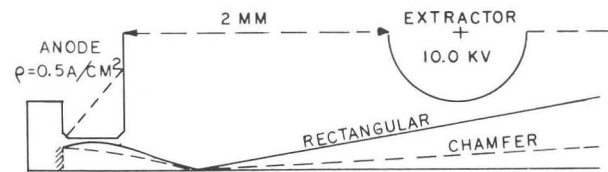


Fig. 10 Beam envelopes for rectangular and chamfered emission slits

For higher initial current densities, lower divergences can be expected (see Fig. 11).

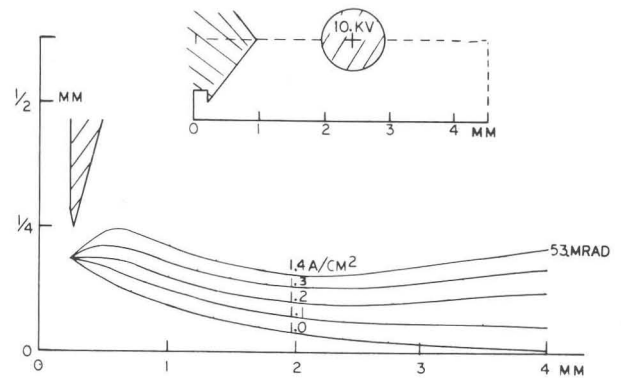


Fig. 11 Beam envelopes for various densities with chamfered emission slit and flat plasma boundary

In practice, only with the Penning source some reduction ( $\sim 75 \text{ mrad}$ ) in angle was observed, but not with the magnetron source. With the Penning source, there was also the tendency of smaller emittance for higher current densities. The different origins of the  $\text{H}^-$  ions in these plasma sources may explain the difference in performance. For the magnetron, the  $\text{H}^-$  ion originates from the cathode and may or may not transfer its electron to a slow hydrogen atom. The ion boundary is, therefore, mainly determined by the shape of the cathode and the divergence is not affected by the shape of the anode slit. A concave cathode in the magnetron may improve the optics of the extracted beam. For the Penning source, the  $\text{H}^-$  ions are formed in the plasma and,

therefore, there is some kind of plasma boundary which will be shaped by the field gradient. Therefore, the flat boundary in Fig. 10 and Fig. 11 is in reality probably concave so that cross-over of the beam in the extraction gap can always be expected.

The beam performance of the Penning source is, in general, better than the magnetron. Its emittance is smaller, in particular for high emission current densities. As mentioned earlier, lower divergence can be obtained by chamfering the source emission slit. The density distribution along the slit is also more uniform than in the magnetron. This is observed both in the emittance measurements and by visual inspection. It should be noticed that the Penning mode of operation is obtained with high ( $5\text{ kW/cm}^2$ ) cathode power density.

The emittances in the direction parallel to the slit(s) (Fig. 4, and Fig. 7) show no important space-charge blow-up; the beam size increased only by a few millimeters across a drift of 8 cm. The split in the middle of the emittance in Fig. 4 is caused by a metal bar in the center of the emission slit. The split remained even after an 8 cm drift of the beam, confirming the negligible space-charge forces in that part of the beam. The aberrations of the emittances in the direction of the slits are probably caused by misalignment of the electrodes and the off-axis, non-uniform magnetic field. In general, emittances were cleaner with low magnetic field. With identical fields in the bending and source magnet, these aberrations can be expected to be reduced significantly.

The operation of the Penning source with low magnetic field (600 Gauss) and high magnetic field (1100 Gauss) allowed mass analysis of the emerging beam and separation of the emittance of the negative hydrogen ion from that of the heavy ion ( $\text{O}^-$  or  $\text{OH}^-$ ), as demonstrated in Fig. 4. The proportion of heavy ions in the beam can be large in an unconditioned source. When the source is baked out properly, the heavy ion part of the beam practically disappears.

When hydrogen gas was replaced with deuterium gas, the same beam parameters (current densities and emittances) could be achieved. With deuterium, the source preferred to operate at higher magnetic field and higher ignition voltage, resulting in high arc currents.

With improved electrode alignments, higher extraction voltages, and with the source magnetic field the same as in the beam transport magnet, the matching of high current negative ion beams to the high voltage accelerator looks very promising.

#### Reference

- 1 Omibyete Corporation.